Anal. Chem. **2009,** *81,* 4831–4839

Multiplex Charge-Transfer Interactions between Quantum Dots and Peptide-Bridged Ruthenium Complexes

Igor L. Medintz,*,† Dorothy Farrell,‡ Kimihiro Susumu,‡ Scott A. Trammell,† Jeffrey R. Deschamps,§ Florence M. Brunel,|| Philip E. Dawson,|| and Hedi Mattoussi*,‡

Center for Bio/Molecular Science and Engineering, Code 6900, Division of Optical Sciences, Code 5611, Laboratory for the Structure of Matter, Code 6030, U.S. Naval Research Laboratory, Washington, DC 20375, and Departments of Cell Biology and Chemistry and the Skaggs Institute for Chemical Biology, The Scripps Research Institute, La Jolla, California 92037

Simultaneous detection of multiple independent fluorescent signals or signal multiplexing has the potential to significantly improve bioassay throughput and to allow visualization of concurrent cellular events. Applications based on signal multiplexing, however, remain hard to achieve in practice due to difficulties in both implementing hardware and the photophysical liabilities associated with available organic dye and protein fluorophores. Here, we used charge-transfer interactions between luminescent semiconductor quantum dots (QDs) and proximal redox complexes to demonstrate controlled quenching of QD photoemission in a multiplexed format. In particular, we show that, because of the ability of the Ru complex to effectively interact with CdSe–ZnS QDs emitting over a broad window of the optical spectrum, higher orders of multiplexed quenching can be achieved in a relatively facile manner. Polyhistidine-appended peptides were site-specifically labeled with a redox-active ruthenium (Ru) phenanthroline complex and self-assembled onto QDs, resulting in controlled quenching of the QD emission. Different QD colors either alone or coupled to Ru–phen–peptide were then mixed together and optically interrogated. Composite spectra collected from mixtures ranging from four up to eight distinct QD colors were deconvoluted, and the individual QD photoluminescence (PL) loss due to charge transfer was quantified. The current multiplexing modality provides a simpler format for exploiting the narrow, size-tunable QD emissions than that offered by resonance energy transfer; for the latter, higher orders of multiplexing are limited by spectral overlap requirements.

The introduction of luminescent semiconductor nanocrystals or quantum dots (QDs) to biology has provided researchers with novel fluorescent tools for potentially achieving advances in imaging, sensing, and for developing optical barcodes.[1–3] This arises from the unique photophysical properties that these fluorophores provide including size-tunable narrow, symmetrical photoluminescence (PL, full width at half-maximum ~25–40 nm) and broad absorption spectra that continuously increase toward shorter wavelengths.[1,4] With the use of different semiconductor combinations it is possible to prepare nanocrystals with emissions ranging from the UV to well into the near-infrared (NIR) region of the optical spectrum. QDs also exhibit high quantum yields, a pronounced resistance to chemical degradation, and high photobleaching thresholds.[1] Perhaps most importantly, multiple QDs present in the same sample can be efficiently excited at a single wavelength far removed (>100 nm) from their respective emissions. This makes QDs directly amenable to signal multiplexing, i.e., the simultaneous detection of multiple concurrent fluorescent emissions or channels.

Fluorescence multiplexing using QDs has already been demonstrated in several biosensing formats. These include (1) use of four-color QD–antibody immunoconjugates to simultaneously detect four toxins in the same sample,[5] (2) multicolor array hybridization,[6] and (3) eight-color QDs mixed with other fluorophores were utilized in polychromatic flow cytometry immunophenotyping assays.[7] QDs have also been encapsulated within carrier particles to create multicolor optically barcoded probes. These have been used in preliminary demonstrations, such as the detection of DNA hybridization and the screening of multiple protein binding events,[3,8] quantitative monitoring of gene expres-

* To whom correspondence should be addressed. E-mail: Igor.medintz@nrl.navy.mil (I.L.M.); Hedi.mattoussi@nrl.navy.mil (H.M.).

† Center for Bio/Molecular Science and Engineering, U.S. Naval Research Laboratory.

‡ Division of Optical Sciences, U.S. Naval Research Laboratory.

§ Laboratory for the Structure of Matter, U.S. Naval Research Laboratory.

|| The Scripps Research Institute.

(1) Michalet, X.; Pinaud, F. F.; Bentolila, L. A.; Tsay, J. M.; Doose, S.; Li, J. J.; Sundaresan, G.; Wu, A. M.; Gambhir, S. S.; Weiss, S. *Science* **2005**, *307*, 538–544.

(2) Klostranec, J. M.; Chan, W. C. W. *Adv. Mater.* **2006**, *18*, 1953–1964.

(3) Han, M.; Gao, X.; Su, J. Z.; Nie, S. *Nat. Biotechnol.* **2001**, *19*, 631–635.

(4) Murray, C. B.; Kagan, C. R.; Bawendi, M. G. *Annu. Rev. Mater. Sci.* **2000**, *30*, 545–610.

(5) Goldman, E. R.; Clapp, A. R.; Anderson, G. P.; Uyeda, H. T.; Mauro, J. M.; Medintz, I. L.; Mattoussi, H. *Anal. Chem.* **2004**, *76*, 684–688.

(6) Shepard, J. R. E. *Anal. Chem.* **2006**, *78*, 2478–2486.

(7) Chattopadhyay, P. K.; Price, D. A.; Harper, T. F.; Betts, M. R.; Yu, J.; Gostick, E.; Perfetto, S. P.; Goepfert, P.; Koup, R. A.; De Rosa, S. C.; Bruchez, M. P.; Roederer, M. *Nat. Med.* **2006**, *12*, 972–977.

(8) Olivos, H. I.; Bachhawat-Sikder, K.; Kodadek, T. *ChemBioChem* **2003**, *4*, 1242–1245.

10.1021/ac900412j CCC: $40.75
Published on Web 05/15/2009

sion levels,[9] and in one-bead−one-compound deacetylase enzyme screening assays.[10] Beyond applications in sensor development, preliminary reports have shown the potentials of using QDs to develop QD-emission-based cryptograms, where the number of QD emissions, their relative intensities, along with the choice of excitation wavelength could provide a unique approach to data encryption.[11]

We have previously shown that fluorescence resonance energy transfer (FRET) in a multiplexed format is easier to implement using a configuration where several QD donors interact with the same dye acceptor.[12] Sample configurations with up to four QD FRET channels were realized. We found that the PL loss for each QD color traced the FRET efficiency in that QD−acceptor channel, and this depended on the corresponding spectral overlap, the donor−acceptor separation distance, and the number of acceptors interacting with the donor (conjugate valence). Although this strategy has been demonstrated for detecting mixed hybridization,[13] the range of FRET channels in a mixed sample is limited to those offering sizable donor−acceptor spectral overlap and optically resolvable individual QD emissions.

Recently, we characterized the charge-transfer interactions between ruthenium phenanthroline (Ru−phen) and CdSe−ZnS QD conjugates assembled via a peptide bridge.[14] The Ru−phen-labeled peptides were ratiometrically self-assembled onto the QDs, and the resulting quenching was analyzed. Our data showed that effective quenching of the QD PL by the proximal Ru−phen complex can occur for several size nanocrystals emitting over a broad window of the optical spectrum. Results also showed that PL quenching efficiency directly traced the number of Ru−phen complexes brought into proximity of the QD. We attributed the PL loss to charge transfer from the metal complex to primarily the surface states of the QDs and further demonstrated that this process is controlled by the mismatch between the oxidation levels of the metal complex and the nanocrystals. Other metal complexes such as ferrocence exhibiting higher oxidation potentials than that of the QDs did not engage in charge-transfer interactions and did not induce PL quenching.[14] These results suggested that exploiting charge transfer as a transduction mechanism, where many distinct QD colors/sizes are efficiently quenched by the same Ru−phen complex acting as a "universal" quencher, could improve the multiplexing capabilities of QDs as compared to configurations offered by FRET. To demonstrate a viable framework for this, a maleimide-functionalized Ru−phen complex was attached to the terminal end of a polyhistidine-appended peptide and self-assembled onto the QDs. Several distinct QD colors conjugated with controlled numbers of Ru−phen−peptide (hence quenched to a desired level) were mixed and optically interrogated, see schematic in Figure 1. The individual signature of each QD color in the mixture was deconvoluted, analyzed, and the PL loss was compared to that of the QD control alone. Up to eight distinct interaction channels were successfully analyzed.

MATERIALS AND METHODS

Quantum Dots. CdSe−ZnS core−shell QDs with emission maxima centered at 510, 537, 555, 565, 581, 590, 610, and 635 nm were used (see Figure 2). The nanocrystals were synthesized by reacting organometallic precursors in a hot coordinating solvent mixture following the procedures described in refs 15 and 16. The 635 nm emitting nanocrystals were synthesized with a two-layer shell structure made of CdZnS−ZnS. Extinction coefficients were estimated as described.[17,18] QDs were made hydrophilic by exchanging the native trioctyl phosphine and trioctyl phosphine oxide (TOP/TOPO) ligands with either dihydrolipoic acid (DHLA) or poly(ethylene glycol) (PEG)-appended DHLA; PEG with $M_W \sim 600$ Da was used, see Figure 1b for structures.[19,20] The resulting nanocrystals are referred to as DHLA-QDs and DHLA−PEG-QDs, respectively.

Peptide Labeling. The synthetic peptide sequence used for this study consisted of the generic sequence Ac-$(His)_6$GlyLeuAibAlaAlaGlyGlyHisTyrGlyCys-amide, where Ac is an acetyl group at the N-terminus and Aib is the noncoded residue α-amino isobutyric acid. The peptides were synthesized manually using in situ neutralization cycles for Boc solid-phase peptide synthesis.[21,22] Maleimido-functionalized tetraamine ruthenium Ru(II) polypyridyl complex, $[Ru(II)(NH_3)_4$(1,10-phenanthroline-5-maleimide)$](PF_6)_2$ (referred to as Ru−phen, synthesized as detailed in ref 23), was reacted with the terminal cysteine of the peptide to form the covalently labeled Ru−phen peptide complex.[14] Briefly, 1 mg of peptide was dissolved in 1 mL of PBS (0.1 M sodium phosphate and 0.15 M NaCl pH 7.4) along with 1 mg of Ru−phen maleimide and incubated overnight at 4 °C with continuous agitation. Labeled peptide was purified over Ni−NTA resin (Qiagen, Valencia CA), eluted with 250 mM imidazole−PBS, dialyzed against PBS, and desalted using reversed-phase 18 oligonucleotide purification cartridges (Applied Biosystems Incorporated, Mountain View, CA).[22] Labeled peptide concentration was determined using the Ru−phen complex absorbance at 490 nm (molar extinction coefficient 5000 M^{-1} cm^{-1}). Purified peptides were lyophilized and stored at −20 °C until used.

Conjugate Preparation and Fluorescence Data Collection. Each set of QD−Ru−phen peptide conjugate was independently formed by adding the indicated molar ratios of Ru−phen−peptide

(9) Eastman, P. S.; Ruan, W. M.; Doctolero, M.; Nuttall, R.; De Feo, G.; Park, J. S.; Chu, J. S. F.; Cooke, P.; Gray, J. W.; Li, S.; Chen, F. Q. F. *Nano Lett.* **2006**, *6*, 1059–1064.
(10) Garske, A. L.; Denu, J. M. *Biochemistry* **2006**, *45*, 94–101.
(11) Zhou, M.; Chang, S.; Grover, C. P. *Opt. Express* **2004**, *12*, 2925–2931.
(12) Clapp, A. R.; Medintz, I. L.; Uyeda, H. T.; Fisher, B. R.; Goldman, E. R.; Bawendi, M. G.; Mattoussi, H. *J. Am. Chem. Soc.* **2005**, *127*, 18212–18221.
(13) Algar, W. R.; Krull, U. J. *Anal. Chim. Acta* **2007**, *581*, 193–201.
(14) Medintz, I. L.; Pons, T.; Trammell, S. A.; Grimes, A. F.; English, D. S.; Blanco-Canosa, J. B.; Dawson, P. E.; Mattoussi, H. *J. Am. Chem. Soc.* **2008**, *130*, 16745–16756.
(15) Peng, Z. A.; Peng, X. *J. Am. Chem. Soc.* **2001**, *123*, 183–184.
(16) Dabbousi, B. O.; Rodriguez-Viejo, J.; Mikulec, F. V.; Heine, J. R.; Mattoussi, H.; Ober, R.; Jensen, K. F.; Bawendi, M. G. *J. Phys. Chem. B* **1997**, *101*, 9463–9475.
(17) Leatherdale, C. A.; Woo, W. K.; Mikulec, F. V.; Bawendi, M. G. *J. Phys. Chem. B* **2002**, *106*, 7619–7622.
(18) Striolo, A.; Ward, J.; Prausnitz, J. M.; Parak, W. J.; Zanchet, D.; Gerion, D.; Milliron, D.; Alivisatos, A. P. *J. Phys. Chem. B* **2002**, *106*, 5500–5505.
(19) Mattoussi, H.; Mauro, J. M.; Goldman, E. R.; Anderson, G. P.; Sundar, V. C.; Mikulec, F. V.; Bawendi, M. G. *J. Am. Chem. Soc.* **2000**, *122*, 12142–12150.
(20) Susumu, K.; Uyeda, H. T.; Medintz, I. L.; Pons, T.; Delehanty, J. B.; Mattoussi, H. *J. Am. Chem. Soc.* **2007**, *129*, 13987–13996.
(21) Schnolzer, M.; Alewood, P.; Jones, A.; Alewood, D.; Kent, S. B. *Int. J. Pept. Protein Res.* **1992**, *40*, 180–193.
(22) Sapsford, K. E.; Pons, T.; Medintz, I. L.; Higashiya, S.; Brunel, F. M.; Dawson, P. E.; Mattoussi, H. *J. Phys. Chem. C* **2007**, *111*, 11528–11538.
(23) Trammell, S. A.; Goldston, H. M.; Tran, P. T.; Tender, L. M.; Conrad, D. W.; Benson, D. E.; Hellinga, H. W. *Bioconjugate Chem.* **2001**, *12*, 643–647.

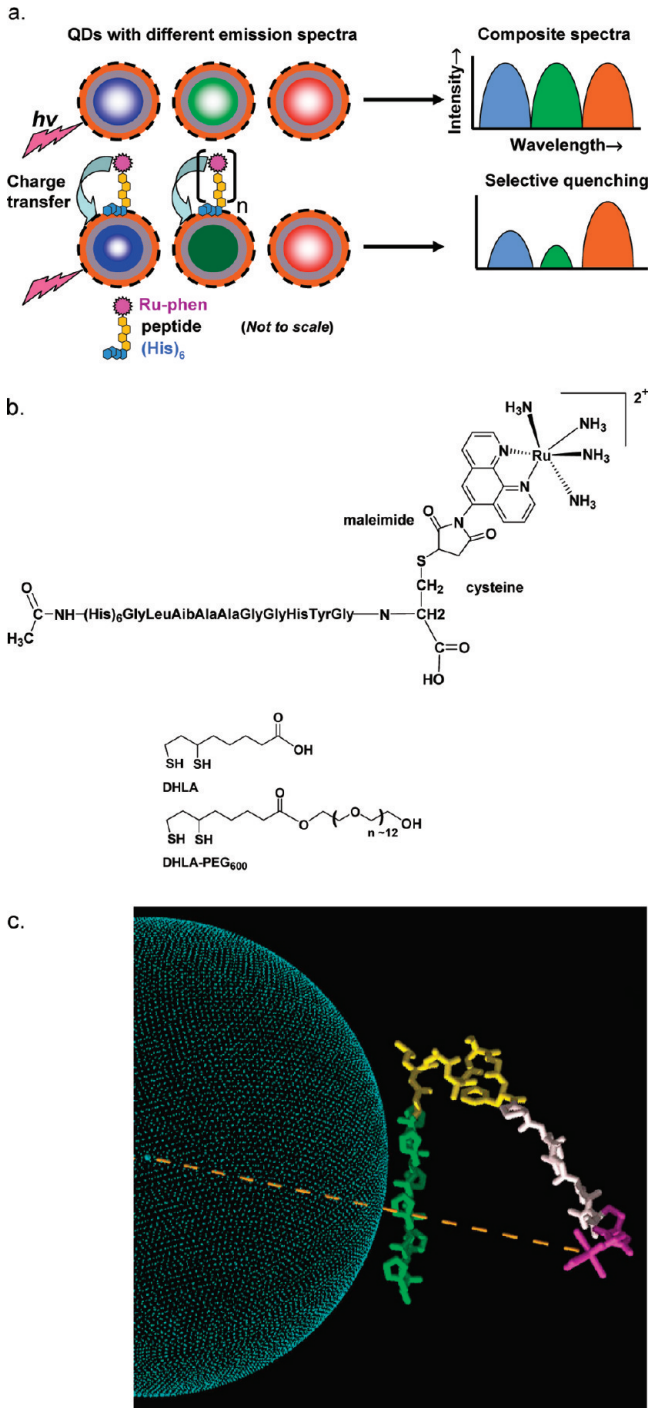

Figure 1. Schematics of the charge-transfer-based multiplexing. (a) Top: CdSe–ZnS core–shell QDs with different emissions are mixed yielding a composite multiplex emission spectrum. Bottom: Self-assembling QD subsets with Ru–phen complex labeled peptide selectively quench their PL emission (via charge transfer). Quenching of each QD color can be further tailored by varying the number of Ru–phen peptides per QD. (b) Structures of Ru(II) polypyridyl maleimide-labeled peptide (all amino acids abbreviated by three-letter code except the labeled cysteine), DHLA, and DHLA–PEG ligands. (c) Simulated structure of a QD self-assembled with one Ru–phen–peptide. The QD is approximated by a sphere of ~58 Å representing the core–shell diameter (λ_{em} ~ 555 nm). The peptide has $(His)_6$—green, GlyLeu-AibAlaAlaGlyGly—yellow, HisTyrGlyCys—white, and the Ru–phen complexes in red. Center-to-center distance of ~53 Å is marked with a dashed line and estimated using FRET with dye-labeled versions of this peptide (refs 22 and 25). Modeling is further described in the Supporting Information.

to the QDs in 100 μL of 10 mM sodium tetraborate buffer pH 9.5 and let to incubate for 1 h. Attachment of the Ru–phen-labeled peptide to the QD surface is driven by metal affinity interactions between the histidine tag and the metal-rich QD surface. This results in a conjugate geometry where each QD of a particular emission color is simultaneously attached to an average number of Ru–phen peptides (QD-conjugate valence). Choosing the conjugate valence allows one to achieve the desired quenching level for each QD population. For multiplex experiments, these independently assembled QD conjugates were then mixed together and simultaneously interrogated. Characterization of each set (color) of self-assembled conjugates with increasing Ru–phen–peptide/QD ratio provided a reference to which the fluorescence of that particular QD contribution in a later mixture could be compared (see Figure 2). The final amounts of QDs used in the mixture ranged from 5 to 40 pmol depending on the quantum yield and the observed quenching efficiency. Individual QD conjugates prepared with the desired quenching levels were mixed and diluted in borate buffer to a final volume of 3 mL (corresponds to a final QD concentration range of ~1.7–13.3 nM). Solutions were then loaded into a 3 mL quartz cuvette (1 cm optical path), and PL spectra were acquired using a SPEX Fluorolog-3 fluorimeter (Jobin Yvon/SPEX, Edison, NJ) with 350 nm excitation.

Spectral Deconvolution. Deconvolution of the composite spectra to isolate the individual contribution of each QD population is critical to the current application. For this, we first fit the PL spectra of each individual QD population (neat solution) to a Gaussian profile.[5,12] Then the composite emission spectrum from each sample mixture consisting of unquenched QDs (no Ru–phen–peptide) was fit using a superposition of Gaussian-like profiles of the form

$$I(\lambda) = \sum_i I_i = \sum_i A_i e^{\frac{-(\lambda-\lambda_i)^2}{\sigma_i^2}} \quad (1)$$

where A_i is constant parameter, i designates an individual population, $I_i(\lambda)$ is its emission spectrum, and A_i is the corresponding peak amplitude. λ_i designates the emission peak location, and σ_i accounts for its width; the latter were extracted from fits to the spectra of each individual QD population. This provided a reference composite spectrum for each QD sample to which the quenched QD–peptide–Ru–phen conjugates were compared. To extract a measure for the PL quenching in the sample mixture we assumed that the Gaussian profiles of each population, $I_i(\lambda)$, was maintained (i.e., λ_i and σ_i stay the same and only the amplitude is reduced) as demonstrated in our previous study.[14] The composite spectrum was then fit to an equation of the form

$$I(\lambda) = \sum_i C_i I_i(\lambda) = \sum_i C_1 A_i e^{\frac{-(\lambda-\lambda_i)^2}{\sigma_i^2}} \quad (2)$$

where C_i is a weighting factor ($0 < C_i < 1$ for all cases) that provided a measure of the PL loss for that QD subset. All fits

(24) Lee, J. A.; Mardyani, S.; Hung, A.; Rhee, A.; Klostranec, J. M.; Mu, Y.; Li, D.; Chan, W. C. W. *Adv. Mater.* **2007**, *19*, 3113–3118.
(25) Medintz, I. L.; Mattoussi, H. *Phys. Chem. Chem. Phys.* **2009**, *11*, 17–45.

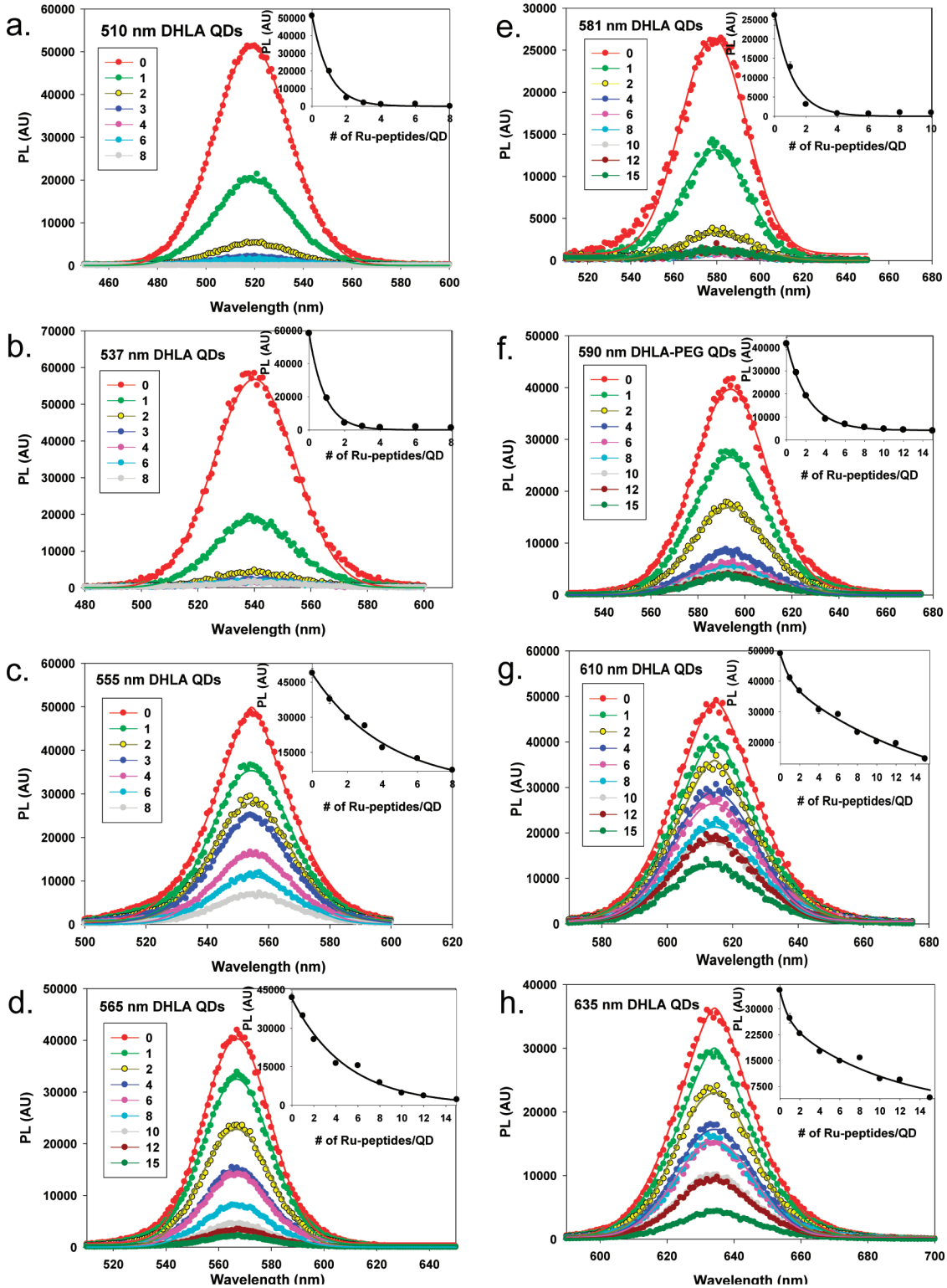

Figure 2. PL of QD−Ru−phen−peptide vs number of Ru complexes per QD. (a−h) PL data are shown for 510, 537, 555, 565, 581, 590, 610, and 635 nm QDs. Both DHLA- and DHLA−PEG-QDs were used. QD emissions were fit with Gaussian-like profiles. Inset shows QD λ_{max} PL intensity vs *n*.

were done using IgorPro software (WaveMetrics, Portland, OR). Gaussian profiles have been previously used for single-population emissions, when fitting the composite spectra collected from an optical barcode made of multiple QD colors embedded in a polymeric bead.[24]

RESULTS AND DISCUSSION

Self-Assembly of Quantum Dot−Ruthenium Phenanthroline-Labeled Peptide Assemblies. We utilize metal-affinity-driven self-assembly to facilitate the conjugation between hexahistidine (His_6)-appended peptides and QD surfaces.[22] This

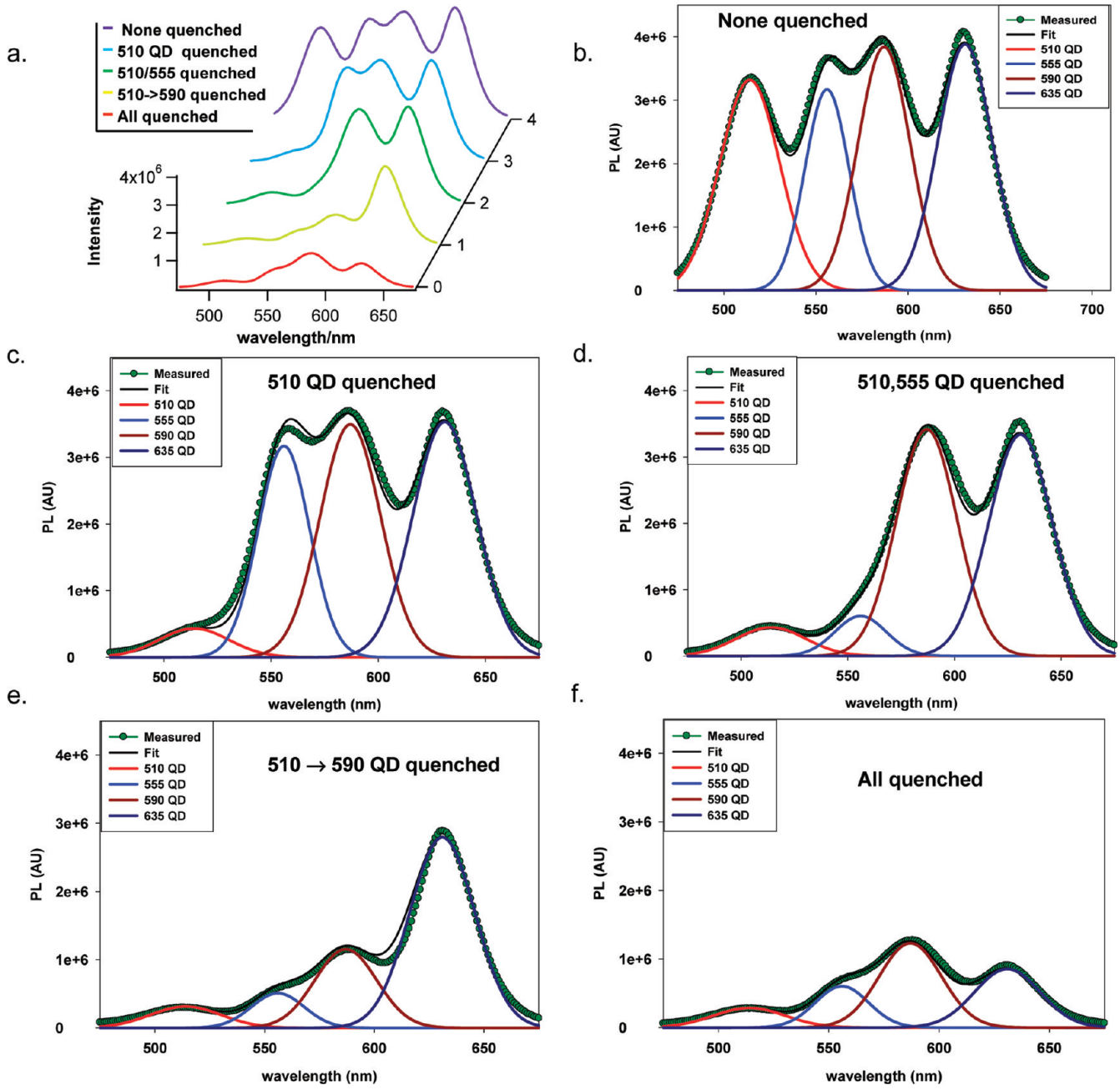

Figure 3. Four-color multiplexing configuration using 510, 555, 590, and 635 nm emitting DHLA−PEG-QDs. (a) Composite spectra for different mixing configurations: none conjugated to Ru−phen−peptide, 510 nm QD, 510 and 555 nm QDs, 510, 555, 590 nm QDs, and all conjugated to Ru−phen−peptide. (b−f) Measured composite, deconvoluted individual QD spectra, and a fit of the summed components for the various configurations from panel a.

conjugation strategy applies to both DHLA- and DHLA−PEG-QDs, has a high affinity with nanomolar dissociation constants, and allows for control over conjugate valence.[22] The peptide sequence we used here as a bridge between the nanocrystals and the Ru−phen complex has key structural characteristics which facilitate its function (see simulated structure shown in Figure 1c). It has a helix-linker sequence (highlighted in yellow) that provides rigidity attached to the N-terminal His_6 QD assembly sequence (green), a spacer (highlighted in white), and a terminal cysteine residue which is site-specifically coupled to the maleimide on the Ru−phen (red). For these experiments, appropriate molar ratios of Ru−phen−peptide were self-assembled onto each set of QDs to achieve the desired PL quenching efficiency prior to mixing with the other QD samples (see the Materials and Methods section for more details).

The charge-transfer interactions from the Ru−phen to the QDs, which effectively quench the PL of QDs emitting across a broad window of the visible spectrum, form the basis of the multiplexing demonstrated here.[14] In the following, we discuss different QD quenching sample configurations: First several QD populations emitting across distinct regions of the optical spectrum were coupled to the Ru−phen−peptide and interrogated individually to show that PL quenching could be controlled through conjugate valence; this extended our previous results and provided an

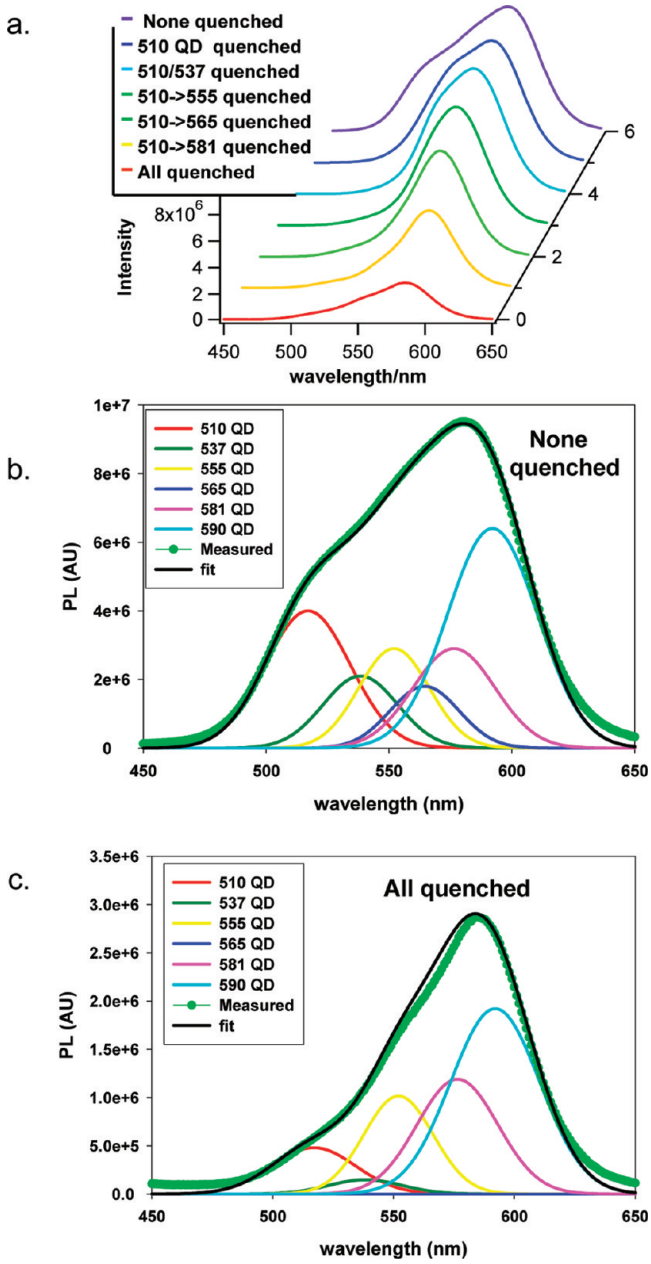

Figure 4. Six-color multiplexing configuration using 510, 537, 555, 565, 581 nm DHLA-QDs and 590 DHLA−PEG-QDs. (a) Evolution of composite spectra collected from different mixing conditions: none conjugated to Ru−phen−peptide; 510 nm QDs; 510 and 537 nm QDs; 510, 537, 555 nm QDs; 510, 537, 555, 565 nm QDs; 510, 537, 555, 565, 581 nm QDs; and all conjugated to Ru−phen−peptide. (b and c) Measured composite, deconvoluted individual QD spectra, and a fit of the summed components for none and all conjugated to Ru−phen−peptide ("all quenched"). Note the different intensity scales in panels b and c.

initial set of reference data (standards). Then mixtures of the QD−Ru−phen−peptide assemblies using varying degrees of complexity and reagent concentrations were simultaneously interrogated. This allowed several multiplex charge-transfer configurations to be investigated.

Quenching of Individual QD Populations: Single-Channel Interactions. Figure 2 shows the progression of the PL spectra collected from eight distinct QD dispersions/colors (peak emission ranging from 510 to 635 nm) self-assembled with increasing numbers of Ru−phen−peptide per QD conjugate. Overall, the data confirm our previous findings that the Ru−phen complex can engage in effective charge-transfer-induced quenching of QD emission, with a PL loss that directly depends on the conjugate valence for each set of QDs.[14] Data also show that smaller QDs exhibit higher quenching efficiencies than their large-size (red-emitting) counterparts. For example, a PL loss exceeding 50% was measured for the 510 nm QDs (core radius ~13.5 Å) at a nominal ratio of one Ru−phen−peptide per QD conjugate, whereas only ~15% PL loss was measured for the 610 nm QDs (core radius ~24 Å) at the same valence. The insets in each panel of Figure 2 show the trend for QD PL loss versus number of Ru−phen complex per conjugate, n, which follows the general form

$$\frac{PL_n}{PL_0} = 1 - \frac{n}{K + n} \qquad (3)$$

where PL_n and PL_0 designate the fluorescence spectra measured for QD−Ru−phen conjugates and QDs alone, respectively, and K reflects the center-to-center separation distance r (assumed constant for all self-assembled conjugates).[14] This quenching behavior is very similar to what was recorded for FRET data collected from QD−peptide/protein−dye conjugates (QD−dye pairs).[25] The more pronounced quenching for smaller size (bluer emitting) QDs may be attributed to a higher density of surface states and higher probability for charge transfer than that expected for their larger size counterparts.[14] More importantly, because the PL loss for a given QD color directly depends on n, the desired level of quenching can be achieved by discretely controlling the conjugate valence.

Four-Channel Interactions. In the first multiplex configuration tested we employed four sets of QDs having well-resolved emissions (limited spectral overlap or cross-talk): 510, 555, 590, and 635 nm emitting DHLA−PEG-QDs (see Figure 3). Concentrations of the various sets of QDs in the mixture were adjusted depending on their relative PL emissions to provide comparable contributions (same order of magnitude) to the measured composite spectra. Bluer emitting dots have lower extinction coefficients than redder emitting ones; thus, slightly larger reagent concentrations were needed for the smaller size nanocrystals to compensate for this difference. A series of samples with different combinations of unconjugated QDs and/or QD−Ru−phen−peptide assemblies were then prepared using the four QD colors. In these samples, the ratio of Ru−phen-to-QD used for each set was adjusted so that a sizable and easy to quantify PL loss (~50−70%) could be realized; ratio selection was guided by the data shown in Figure 2. This provided an unambiguous evaluation of each quenching channel, and this level of PL loss was maintained for subsequent configurations. Figure 3a shows the experimental spectra collected for several combinations of QD mixtures, namely, no QD set conjugated to Ru−phen−peptide, one-, two-, three-, and all four-color QDs conjugated to the Ru−phen complex. In the mixed samples, the emission peak of each QD set can still be identified due to the clear spectral separation for these sets. For each of these four-channel configurations, the composite spectra along with the deconvoluted individual contribution of each QD population and a resummation of the individual fits are shown in Figure 3b−f.

We should emphasize that PL quenching of CdSe−ZnS QDs by proximal Ru complex coupled via the His-appended peptide

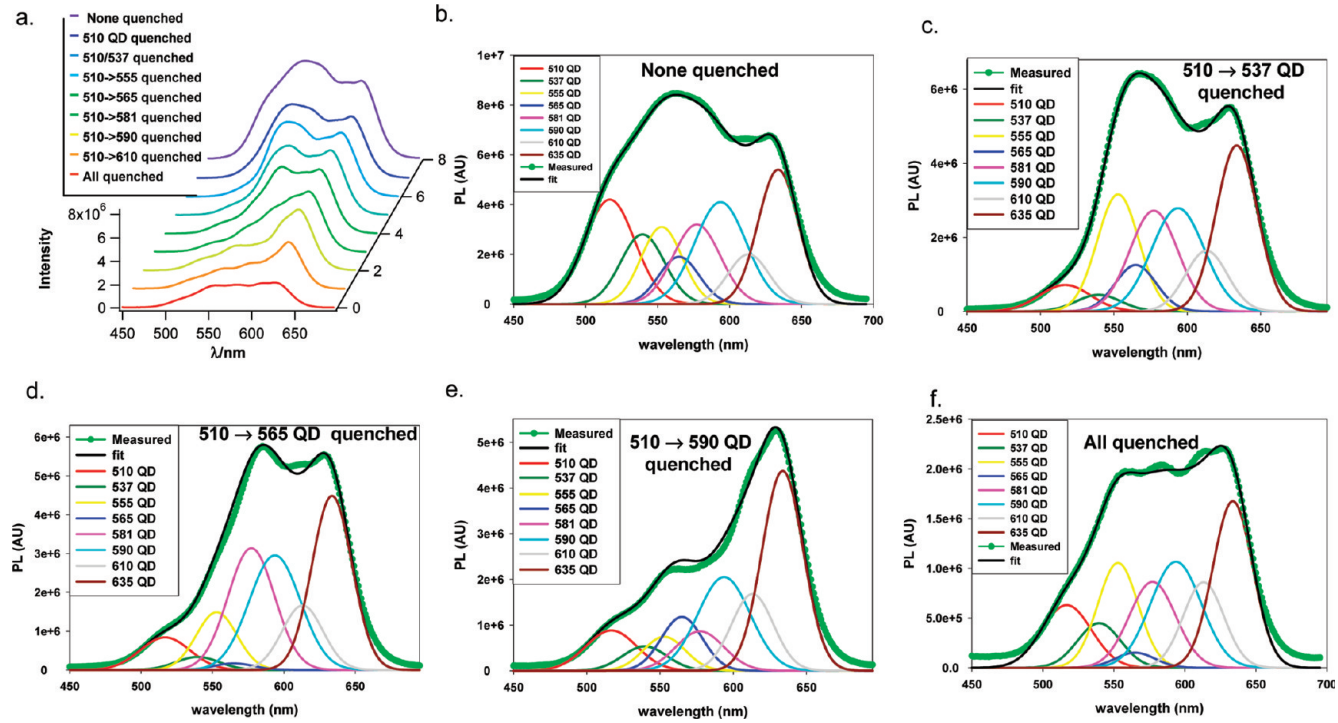

Figure 5. Eight-color multiplexing configuration using 510, 537, 555, 565, 581, 590, 610, and 635 nm QDs. (a) Evolution of composite spectra collected from different mixing conditions: none; 510 nm QDs; 510 and 537 nm QDs; 510, 537, 555 nm QDs; 510, 537, 555, and 565 nm QDs; 510, 537, 555 565, and 581 nm QDs; 510, 537, 555 565, 581, and 610 nm QDs; and all conjugated to Ru−phen−peptide. Measured composite, deconvoluted individual QD spectra, and a fit of the summed components for none (b); 510 and 537 nm QDs quenched (c); 510 through 565 nm QDs quenched (d); 510 through 590 nm QDs quenched (e); and all quenched (f). Note the different intensity scales for panels b−f.

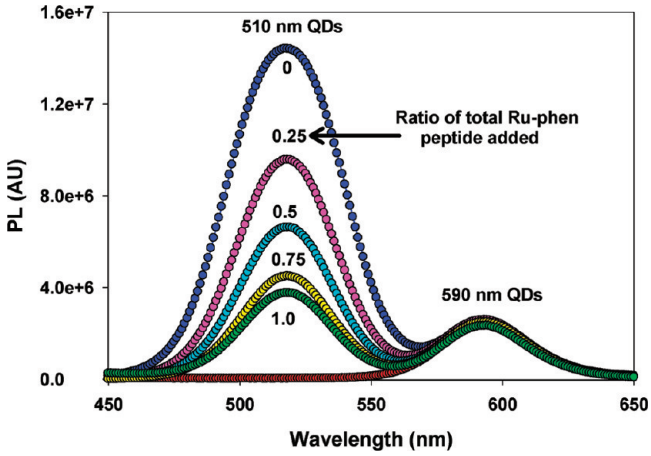

Figure 6. Evaluation of solution-phase quenching. The PL of 590 nm QDs was monitored in the presence of 510 nm QDs preassembled with an increasing molar ratio of Ru-labeled peptide. For the highest value of 1, the molar amount of Ru−phen−peptide added to the 510 nm QDs is equivalent to the total concentration used in the eight-plex sample (see Figure 5). Fractions indicate incremental amounts of total Ru−phen−peptide added to the 510 nm QDs.

bridges was measured using nanocrystals capped with either DHLA or DHLA−PEG. Data and fits for a similar four-plex configuration using 510, 555, 590, and 635 nm emitting DHLA-QDs provided essentially equivalent data to the above (Supporting Information). An alternate four-plex sample configuration using a different set of QDs, namely, 510, 537, 555, and 565 nm emitting QDs, was also tested; the peak emissions of these populations are much closer than those described above, and individual emission maxima were no longer visibly delineated. Deconvolution of the composite spectra to isolate individual QD contributions, however, could still be efficiently achieved (see Supporting Information).

Six- and Eight-Channel Interactions. Figure 4a shows the composite spectra collected from sample mixtures of six QD populations consisting of 510, 537, 555, 565, 581, and 590 nm emitting QDs. In these mixtures, selected subsets were conjugated to Ru−phen−peptide and experienced PL loss. Parts b and c of Figure 4 show the composite spectra, along with the deconvoluted individual PL contributions for two configurations: the "none" and "all" QD populations engaged in charge-transfer quenching, respectively. Figure 5a shows the composite spectra collected from an eight-color mixture (eight-plex) using 510, 537, 555, 565, 581, 590, 610, and 635 nm emitting QDs, where as above selected subsets or all populations were engaged in quenching interactions with the Ru−phen complex. Parts b−f of Figure 5 show the composite spectra collected, along with the deconvoluted individual contributions from each population for samples that had zero, two, four, six, and all eight QD colors coupled to Ru−phen, respectively. Similar data along with the spectral deconvolution were also collected from five- and seven-color QD mixtures (see Supporting Information).

In each sample configuration used, the overall structure of the composite spectra reflects the number of QD populations involved along with the PL loss experienced by each individual channel. For example, in the six-color quenching progression shown in

Figure 4, the composite spectra are characterized by an asymmetric curve dominated by the slightly stronger emissions from the 510 and 590 nm QDs. The contribution from 590 nm QDs dominates the composite spectrum shown in Figure 4c where the 510 nm QDs are more effectively quenched. Data shown in Figures 3−5 clearly show that quantitative spectral deconvolution of composite spectra which account for the contribution of each QD population can be achieved using eq 2. This also indicates that simultaneous and selective interrogation of single or combinations of charge-transfer channels using these types of QD assemblies can be achieved in a relatively straightforward and selective manner.

Error Analysis. It is important to note that spectral deconvolution in the above examples was simplified by the narrow and symmetric photoemission of the QDs. Nonetheless, errors associated with solution-phase quenching (cross-talk) and the possibility that a particular spectral deconvolution may not be a "unique" solution can affect the subsequent data analysis. These issues become more relevant for higher degrees of complexity (i.e., higher orders of multiplexing), and they could limit the ability to accurately perform spectral deconvolution and extract the quenching efficiency for particular channel(s). "Cross-talk" which arises from collision encounters due to conjugate diffusion is expected to be more pronounced for higher reagent concentrations and/or higher orders of multiplexing.[26] For the latter the overall reagent concentration unavoidably increases even though concentrations of the individual populations may actually be very small. The error associated with the spectral deconvolution is not experimentally induced. It occurs when a solution for the contribution from each QD set in the mixture is not "unique" and a slight adjustment in the relative amplitudes of two or more closely positioned peaks (C_iA_i in eq 2) can produce the same overall fit for a given composite spectrum.

To evaluate the errors associated with solution-phase quenching, we monitored the PL of 590 nm QDs in a mixture with 510 nm QD−Ru−phen−peptide conjugates. The 590 nm QD concentration was identical to the one used in the eight-plex sample described above (Figure 5), whereas that of the 510 nm QDs was higher and matched the concentration of the other seven QD colors combined. The clear spectral separation allowed direct monitoring of the quenching of both QD emissions without signal deconvolution. The molar concentration of Ru−phen peptide preassembled on the 510 nm QDs added to the mixture was incrementally increased until it matched the combined concentration of Ru−phen complex utilized in the above eight-plex (it is equal to the total Ru−phen present for all eight QD colors combined). Data shown in Figure 6 indicate that, whereas PL loss for the 510 nm QDs reached ∼80% (for the highest Ru−phen valence), loss in the 590 nm QD PL was lower than 5%, confirming that the effects of solution-phase collision quenching are overall small. This observation is further complemented by analyzing each deconvoluted QD emission (from the composite spectrum) and comparing it to the emission collected from that same population alone (controls of similarly unquenched or quenched QDs); we found that the difference in PL intensity was less than 10% in all cases. Cumulatively, these results also confirm that there is no visible peptide loss/exchange for these solution conjugates even in concentrated or dense multiplexed formats.

Additional sources of errors can arise from repetitive or sampling error and instrumental uncertainly that do not always cancel each other out but rather obey the summed rule:

$$\text{total error} = (\text{sampling}^2 + \text{instrument}^2 + \text{fitting}^2 + ...)^{1/2} \quad (4)$$

This implies that the largest error tends to dominate the final analysis. We first evaluated the deconvolution or data fitting error for the four-color mixture using 510, 555, 590, and 635 nm DHLA−PEG-QDs (Figure 3). Estimate of the fitting error was derived by comparing the deconvoluted individual spectra (extracted from the composite fit) to controls measured separately for each "unquenched" or "quenched QD" dispersion in a particular mixture. A maximum of ∼5% error was derived for this fitting process. In comparison, instrument error (repetitive analysis and comparison of identical samples) was ∼1%, whereas error associated with sampling was ∼2%. This suggests that when using four well-resolved QD colors, the expected cumulative error affecting deconvolution of a particular population contribution should be ∼5%. To estimate the fitting error arising in more complex configurations, we compared deconvoluted spectra to the measured individual samples for the high-density eight-plex mixture (i.e., 510, 537, 555, 565, 581, 590, 610, and 635 nm QDs). The significant overlap between emissions of the 537, 555, 565, and 581 nm QDs in particular increased the fitting error to ∼20% for the most closely spaced peaks. It is important to note that these fitting errors can be substantially reduced by selecting lower orders of mixing or utilizing a set of well-resolved QD emissions. The use of an alternate more refined and more powerful spectral deconvolution algorithm could also improve fitting and reduce errors. Related to the latter, a similar multi-Gaussian deconvolution method specifically designed for QD bead-based barcodes has been recently described.[24] However, the complexity of codes deconvoluted experimentally was limited to three well-resolved QD colors.

CONCLUSIONS

We exploited the charge-transfer interactions between luminescent QDs and proximal metal/redox complexes to induce controlled quenching of the QD emission in a multiplexed format. Taking advantage of the ability of Ru−phen complex to effectively quench the emission of several size CdSe−ZnS QDs emitting over a broad window of the optical spectrum, we achieved high orders of multiplexed quenching. Indeed our experiments showed that up to eight individual optical channels could be resolved using QD emissions ranging from 510 to 635 nm conjugated to Ru−phen complex via a short peptide bridge. We showed that the relative contribution of each QD color could be extracted from the composite spectra of the solution mixtures having various combinations of QDs and QD−Ru−phen conjugates. This study extended our earlier QD multiplexing studies where either direct fluorescence emission was used to detect four toxins in a mixed sandwich immunoassay[5] or simultaneous FRET interactions in QD−protein−dye assemblies was demonstrated.[12] However, the present multiplexing scheme provides a key advantage, as FRET-

(26) Lakowicz, J. R. *Principles of Fluorescence Spectroscopy*; Springer: New York, 2006.

based multiplexing is limited by the number of suitable QD−dye donor−acceptor pairs. Additionally, the latter type of FRET configuration can become complex when the dye acceptor used is also emissive.[12]

The present QD multiplexing modality can be incorporated into a number of different biosensors and allows for multiplex discrimination of analytes in mixed samples. In our previous report characterizing QD−Ru−phen peptide interactions, we demonstrated that this mechanism could be utilized to monitor the proteolytic activity of several enzymes.[14] Benson's lab has also combined the same QD−Ru quenching with several ligand-binding proteins or aptamers to create biosensors targeting the sugar maltose,[27] fatty acids,[28] lead,[29] or alternatively the enzyme thrombin.[30] A report describing the utilization of QD quenching with slightly different ruthenium complexes for detecting DNA hybridization has also been recently reported.[31] Simultaneously monitoring different proteases, different DNA molecular beacons, or alternatively detecting multiple small molecules utilizing biosensors based upon this interaction may prove to be useful and a logical extension in this work. These types of multiplex sensing formats are highly desirable as they do not suffer from the same photophysical liabilities (i.e., overlapping absorptions/emissions, need for multiple excitation wavelengths/spectra, high cross-talk, etc.) when attempting multiplexing with conventional organic or fluorescent protein fluorophores.[25] In a multiplexed format, when a target molecule specific to one of the sensors is introduced, changes in the PL signal of that channel will be measured, providing a means to sense that particular target(s) presence.

This quenching scheme also suggests the basis for designing multicolor fluorescent barcodes. This can be achieved, for example, by embedding a combination of the QD−Ru−phen peptides into a porous bead, where the emission profile per bead can be controlled to provide a well-defined code. In contrast to current strategies for QD barcoding where individual intensities in the composite are altered by changing a particular QDs concentration,[3,32] charge-transfer-based quenching can allow an orthogonal format where QD concentrations are kept constant and individual emissions are discretely modulated as desired. This may provide an alternate method for generating large sets of predefined spectral codes. For example, in a eight-plex utilized at just four different intensities per QD color, 65 535 possible codes are theoretically possible (m QD colors at n intensities yields $n^m - 1$ codes).[3] Overall, it is clear that, as more of the unique properties available to QDs are elucidated (as exemplified by the coupling of charge transfer for high-order signal multiplexing here), new opportunities will be afforded for enhanced biological analysis.

ACKNOWLEDGMENT

The authors acknowledge ONR, the NRL Nanosciences Institute, and the CB Directorate/Physical S&T Division (DTRA) for financial support. D.F. acknowledges an NRC fellowship through NRL. I.L.M. and D.F. contributed equally to this work

SUPPORTING INFORMATION AVAILABLE

Information including QD−peptide modeling, other multicolor configurations, and their deconvoluted spectra. This material is available free of charge via the Internet at http://pubs.acs.org.

Received for review February 24, 2009. Accepted April 21, 2009.

AC900412J

(27) Sandros, M. G.; Gao, D.; Benson, D. E. *J. Am. Chem. Soc.* **2005**, *127*, 12198–12199.
(28) Aryal, B. P.; Benson, D. E. *J. Am. Chem. Soc.* **2006**, *128*, 15986–15987.
(29) Shete, V. S.; Benson, D. E. *Biochemistry* **2009**, *48*, 462–470.
(30) Swain, M. D.; Octain, J.; Benson, D. E. *Bioconjugate Chem.* **2008**, *19*, 2520–2526.
(31) Zhao, D.; Chan, W. H.; He, Z.; Qiu, T. *Anal. Chem.* **2009**, *81*, 3537–3543.
(32) Fournier-Bidoz, S.; Jennings, T. L.; Klostranec, J. M.; Fung, W.; Rhee, A.; Li, D.; Chan, W. C. W. *Angew. Chem., Int. Ed.* **2008**, *47*, 5577–5581.